PRAMANA
— journal of
physics

Vol. 59, No. 3
September 2002
pp. 497–514

Atomic displacements in dilute alloys of Cr, Nb and Mo

HITESH SHARMA[1] and S PRAKASH[2]
[1]Department of Physics, Panjab University, Chandigarh 160 014, India
[2]Jiwaji University, Gwalior, M P 474 011, India

MS received 12 November 2001; revised 16 February 2002

Abstract. Kanzaki lattice static method is used to calculate the atomic displacements due to substitutional impurities in 3d (Cr) and 4d (Nb, Mo) metals. Wills and Harrison interatomic potential is used to calculate dynamical matrix and the impurity-induced forces up to second nearest neighbors. The calculated atomic displacements for 3d, 4d and 5d impurities in Cr (V, Mn, Fe, Ni, Nb, Mo, Ta and W), Nb (V, Cr, Mn, Fe, Zr, Mo, Ta and W) and Mo (V, Cr, Mn, Fe, Zr, Nb, Ta and W) are tabulated up to 10 NN's. The strain field due to 3d impurities is least in Cr metal while it is larger in Nb and Mo metals. For 4d and 5d impurities the strain is larger in Cr metal than in Nb and Mo hosts. Similar trend is found for relaxation energies also.

Keywords. Strain field; dilute alloys; Kanzaki method.

PACS Nos 63.43.-j; 61.72.-y; 61.72.Ji; 61.43.-j; 61.72.Bb

1. Introduction

Since the early days of spaceflight niobium and molybdenum metals and their alloys have been used in high-temperature propulsion systems [1]. Chromium plating is used to harden steel and prevent its corrosion. The physical properties of these metals are greatly influenced by the structural defects and impurities. The NbZr alloys are used to make superconducting magnets [2]. Molybdenum metal and its alloys due to their strength at high temperature, excellent thermal conductivity and low coefficient of thermal expansion are widely used in electrical and electronic devices, for glass manufacturing, high-temperature furnaces and aerospace equipments [3]. The existence of transition metal impurities in these metals are very common and these impurities affect the physical properties of these metals. Therefore, it has been found interesting to investigate the atomic displacements and relaxation energies due to transition metal impurities in Cr, Nb, and Mo hosts.

Earlier we had extended the Kanzaki lattice static method for bcc metals [4,5] and studied the strain field and electrical field gradients due to impurities in vanadium [4] and iron [6]. The effective ion–ion interaction potential due to Wills and Harrison [7] was used to calculate the Kanzaki forces. The calculated atomic displacements and electric field gradients were found in good agreement with the experimental data. In this paper we use the same formalism to calculate atomic displacements and relaxation energies due to 3d, 4d and 5d transitional impurities in Cr, Nb and Mo metals. The paper is organized as follows:

The necessary formalism is given in §2, the calculations and results are presented in §3 and these are discussed in §4.

2. Formalism

For a perfect crystal with self-consistent pair potential $\phi(r)$, the total interaction energy Φ_0 is given as

$$\Phi_0 = \sum_n \phi(\vec{R}_n^0) \tag{1}$$

where $\vec{R}_n^0$ is the equilibrium position of nth host atom. By introducing an impurity at the origin, the lattice is strained, and the host atoms get displaced to new equilibrium positions $\vec{R}_n = \vec{R}_n^0 + \vec{u}(\vec{R}_n^0)$, where $\vec{u}(\vec{R}_n^0)$ is the atomic displacement of the nth NN's of impurity. The total potential energy Φ for monatomic lattice in the harmonic approximation for this configuration is given as

$$\Phi = \Phi_0 - \sum_{n,\alpha} u_\alpha(\vec{R}_n^0) F_\alpha(\vec{R}_n^0) + \frac{1}{2}\sum_{n,\alpha}\sum_{n',\beta} u_\alpha(\vec{R}_n^0) u_\beta(\vec{R}_{n'}^0)\phi_{\alpha\beta}(n,n') \tag{2}$$

where the force components

$$F_\alpha(\vec{R}_n^0) = -\left.\frac{\partial\Phi}{\partial u_\alpha(\vec{R}_n^0)}\right|_{u_\alpha(\vec{R}_n^0)=0} \tag{3}$$

and the force constants

$$\Phi_{\alpha\beta}(n,n') = \left.\frac{\partial^2\Phi}{\partial u_\alpha(\vec{R}_n^0)\partial u_\beta(\vec{R}_{n'}^0)}\right|_{u_\alpha(\vec{R}_n^0)=u_\beta(\vec{R}_{n'}^0)=0}. \tag{4}$$

Here α,β (x,y,z) denote the Cartesian components.

The equilibrium value of $u_\alpha(\vec{R}_n^0)$ is determined by minimizing Φ with respect to displacements, which gives

$$F_\alpha(\vec{R}_n^0) = \sum_{n',\beta} \phi_{\alpha\beta}(n,n') u_\beta(\vec{R}_{n'}^0). \tag{5}$$

Evidently the displacements can be evaluated if $F_\alpha(\vec{R}_n^0)$ and $\phi_{\alpha\beta}(n,n')$ are known. This is conveniently done by expressing eqs (2)–(5) in Fourier space. The Fourier transform of eq. (2) is given as

$$\Phi = \Phi_0 - \sum_{\alpha q} F_\alpha(\vec{q}) Q_\alpha(\vec{q}) + \frac{N}{2}\sum_{\alpha\beta}\sum_q \phi_{\alpha\beta}(\vec{q}) Q_\alpha(\vec{q}) Q_\beta(\vec{q}) \tag{6}$$

where

$$F_\alpha(\vec{q}) = \sum_n F_\alpha(\vec{R}_n^0)\ \exp(\mathrm{i}\vec{q}\cdot\vec{R}_n^0), \tag{7}$$

$$\phi_{\alpha\beta}(\vec{q}) = \sum_{n-n'} \phi_{\alpha\beta}(n-n') \ \exp\left[-\mathrm{i}\vec{q}\cdot(\vec{R}_n^0 - \vec{R}_{n'}^0)\right]. \tag{8}$$

Here N is the number of lattice points in the crystal and $\vec{q}$ is the wave vector. $F_\alpha(\vec{q})$ and $\phi_{\alpha\beta}(\vec{q})$ are the Fourier transforms of $F_\alpha(\vec{R}_n^0)$ and $\phi_{\alpha\beta}(n-n')$, respectively and $Q_\alpha(\vec{q})$ are the Cartesian components of normal coordinates. Minimizing Φ, given in eq. (6), w.r.t. $Q_\alpha(\vec{q})$, one gets the dynamical equation

$$\sum_\beta \left[N\phi_{\alpha\beta}(-\vec{q})Q_\beta(\vec{q}) - F_\beta(\vec{q})\delta_{\alpha\beta}\delta_{-\vec{q},\vec{q}}\right] = 0. \tag{9}$$

With the knowledge of $\phi_{\alpha\beta}(\vec{q})$ and $F_\beta(\vec{q})$, eq. (9) can be solved for $Q_\alpha(q)$ which are related to $\vec{u}(\vec{R}_n^0)$ by the relation

$$u_\alpha(\vec{R}_n^0) = \sum_{\vec{q}} Q_\alpha(\vec{q}) \ \exp(\mathrm{i}\vec{q}\cdot\vec{R}_n^0). \tag{10}$$

For a central potential, the dynamical matrix is written as

$$\phi_{\alpha\beta}(n) = \left.\frac{\partial^2\phi}{\partial r_\alpha \partial r_\beta}\right|_{r=R_n^0} = \frac{R_{n\alpha}^0 R_{n\beta}^0}{|\ \vec{R}_n^0\ |^2}(A_n - B_n + \delta_{\alpha\beta}B_n), \tag{11}$$

where

$$A_n = \left.\frac{\partial^2\phi}{\partial r^2}\right|_{r=R_n^0}, \quad B_n = \left.\frac{1}{|\vec{R}_n^0|}\frac{\partial\phi}{\partial r}\right|_{r=R_n^0}. \tag{12}$$

In the metallic crystal, the ions are screened by the conduction electrons thereby decreasing the ionic potential faster, which exhibit oscillatory behavior at large distances. It has been found that in the d-band metals the screening is large [8–10]. Therefore major contribution to $\phi_{\alpha\beta}(\vec{q})$ and $F_\alpha(\vec{q})$ in these metals is expected to arise from the first few NN's. Including the interactions up to 2NN's, $\phi_{\alpha\beta}(\vec{q})$ for the bcc structure, from (8) and (11) becomes

$$\phi_{\alpha\alpha}(\vec{q}) = \frac{8}{3}(A_1 + 2B_1)\left[1 - \cos\left(\frac{q_\alpha a}{2}\right)\ \cos\left(\frac{q_\beta a}{2}\right)\ \cos\left(\frac{q_\gamma a}{2}\right)\right]$$

$$+4A_2\left[\sin^2\left(\frac{q_\alpha a}{2}\right) + \sin^2\left(\frac{q_\beta a}{2}\right) + \sin^2\left(\frac{q_\gamma a}{2}\right)\right], \tag{13}$$

$$\phi_{\alpha\beta}(\vec{q}) = \frac{8}{3}(A_1 - B_1)\sin\left(\frac{q_\alpha a}{2}\right)\ \sin\left(\frac{q_\beta a}{2}\right)\ \cos\left(\frac{q_\gamma a}{2}\right), \tag{14}$$

where $\alpha \neq \beta \neq \gamma$ and a is the lattice parameter. Similarly, eq. (7) at the 1NN shell of impurity gives

$$F_\alpha(\vec{q}) = \frac{8}{\sqrt{3}}\mathrm{i}F_\mathrm{I}\sin\left(\frac{q_\alpha a}{2}\right)\ \cos\left(\frac{q_\beta a}{2}\right)\ \cos\left(\frac{q_\gamma a}{2}\right), \tag{15}$$

where F_{I} is the force acting on the 1NN site of impurity. Considering the interaction with the 2NN shell, the components of $F(\vec{q})$ are

$$F_\alpha(\vec{q}) = \mathrm{i}2F_{\mathrm{II}}\ \sin(q_\alpha a), \tag{16}$$

where F_{II} is the force at the 2NN site of impurity. With the knowledge of $\phi_{\alpha\beta}(\vec{q})$ and $F_\alpha(\vec{q})$, eq. (9) is solved for $\vec{Q}(\vec{q})$ for radial forces on the 1NN's and 2NN's of impurity using properties of determinants [4]. These values of $\vec{Q}(\vec{q})$ are used in eq. (10), sum is replaced by integration and $\vec{u}(\vec{R}_n^0)$ are calculated for different values of $\vec{R}_n^0$ by using quadrature method for numerical integration.

The forces F_{I} and F_{II} are calculated by lattice static method [11] as given in ref. [4]. These are given as

$$F_\alpha(\vec{R}_n^0) = -\frac{\partial}{\partial u_\alpha(R_n^0)} \sum_{n'} \Delta\phi(|\vec{R}_{n'}|) \tag{17}$$

where

$$\Delta\phi(r) = \phi_{\mathrm{IH}}(r) - \phi_{\mathrm{HH}}(r), \tag{18}$$

$\phi_{\mathrm{HH}}(r)$ and $\phi_{\mathrm{IH}}(r)$ are the host–host and impurity–host interaction potentials respectively. Expanding $\Delta\phi(|\vec{R}_{n'}|)$ in power series of $\vec{u}(\vec{R}_n^0)$, one gets

$$F_\alpha(\vec{R}_n^0) = -\frac{\partial}{\partial r}\Delta\phi\bigg|_{|r|=|\vec{R}_n^0|} - \vec{u}(\vec{R}_n^0)\frac{\partial^2}{\partial r^2}\Delta\phi\bigg|_{|r|=|\vec{R}_n^0|}. \tag{19}$$

We use Wills and Harrison transition metal model potential [7] which is given as

$$\phi_{\mathrm{HH}}(r) = \phi_{\mathrm{HH}}^{\mathrm{FE}}(r) + \phi_{\mathrm{HH}}^{\mathrm{c}}(r) + \phi_{\mathrm{HH}}^{\mathrm{b}}(r), \tag{20}$$

where

$$\phi_{\mathrm{HH}}^{\mathrm{FE}}(r) = Z_{\mathrm{sH}}^2 e^2\ \cosh^2(\kappa r_{\mathrm{ch}})\frac{\exp(-\kappa r)}{r} \tag{21}$$

$$\phi_{\mathrm{HH}}^{\mathrm{c}}(r) = Z_{\mathrm{dH}}\frac{225}{\pi^2}\frac{\hbar^2 r_{\mathrm{dH}}^6}{m r^8} \tag{22}$$

and

$$\phi_{\mathrm{HH}}^{\mathrm{b}}(r) = -Z_{\mathrm{dH}}\left[1 - \frac{z_{\mathrm{dH}}}{10}\right]\left[\frac{12}{n}\right]^{1/2}\frac{28.1}{\pi}\frac{\hbar^2 r_{\mathrm{dH}}^3}{m r^5}. \tag{23}$$

Here $\phi_{\mathrm{HH}}^{\mathrm{FE}}(r)$ is the free electron contribution, $\phi_{\mathrm{HH}}^{\mathrm{c}}(r)$ arises from the shift in the d-band center due to s–d hybridization and $\phi_{\mathrm{HH}}^{\mathrm{b}}$ arises from the finite d-bandwidth. Equations (20)–(23) are generalized to define the impurity–host interaction which is given as [7]

$$\phi_{\mathrm{IH}}(r) = \phi_{\mathrm{IH}}^{\mathrm{FE}}(r) + \phi_{\mathrm{IH}}^{\mathrm{c}}(r) + \phi_{\mathrm{IH}}^{\mathrm{b}}(r) \tag{24}$$

where

$$\phi_{\mathrm{IH}}^{\mathrm{FE}}(r) = Z_{\mathrm{sH}} Z_{\mathrm{sI}} e^2 \cosh(\kappa' r_{\mathrm{cH}})\ \cosh(\kappa' r_{\mathrm{cI}}) \frac{\exp(-\kappa' r)}{r} \tag{25}$$

$$\phi_{\mathrm{IH}}^{\mathrm{c}}(r) = Z_{\mathrm{d}}^{\mathrm{eff}} \frac{225}{\pi^2} \frac{\hbar^2 r_{\mathrm{dH}}^3 r_{\mathrm{dI}}^3}{m r^8} \tag{26}$$

and

$$\phi_{\mathrm{IH}}^{\mathrm{b}}(r) = -Z_{\mathrm{d}}^{\mathrm{eff}} \left[1 - \frac{Z_{\mathrm{d}}^{\mathrm{eff}}}{10}\right] \left[\frac{12}{n}\right]^{1/2} \frac{28.1}{\pi} \frac{\hbar^2 r_{\mathrm{dH}}^{3/2} r_{\mathrm{dI}}^{3/2}}{m r^5}. \tag{27}$$

Here Z_{sI} is the number of s conduction electrons per atom, r_{dI} and r_{cI} are the d-state radius and model-potential core radius of impurity respectively. κ' is the Thomas–Fermi screening length. The variation of the number of the d electrons in the d-band by the introduction of impurity, therefore we define the effective number of d electrons per atom $Z_{\mathrm{d}}^{\mathrm{eff}}$, in an alloy as the weighted average of the number of d electrons in the host and impurity atoms, i.e.,

$$Z_{\mathrm{d}}^{\mathrm{eff}} = C_{\mathrm{H}} Z_{\mathrm{dH}} + C_{\mathrm{I}} Z_{\mathrm{dI}} \tag{28}$$

where Z_{dI} is the number of quasilocalized d electrons per impurity atom and C_{H} and C_{I} are the concentrations of host and impurity atoms respectively.

In the alloying process, there may be a further transfer of electrons to or from the s and d bands, as a result of which the conduction electron charge may redistribute around impurity to screen or unscreen it. However, we asume that these charge transfers are small and the excess interatomic potential due to impurity is

$$\Delta\phi(r) = \Delta\phi^{\mathrm{FE}}(r) + \Delta\phi^{\mathrm{c}}(r) + \Delta\phi^{\mathrm{b}}(r) \tag{29}$$

where

$$\Delta\phi^{\mathrm{FE}}(r) = \frac{Z_{\mathrm{sH}} e^2}{r} [Z_{\mathrm{sI}}\ \cosh(\kappa' r_{\mathrm{cH}})\ \cosh(\kappa' r_{\mathrm{cI}})\ \exp(-\kappa' r) - Z_{\mathrm{sH}} \cosh^2(\kappa r_{\mathrm{cH}})\ \exp(-\kappa r)], \tag{30}$$

$$\Delta\phi^{\mathrm{c}}(r) = \left[Z_{\mathrm{d}}^{\mathrm{eff}} r_{\mathrm{dI}}^3 - Z_{\mathrm{dH}} r_{\mathrm{dH}}^3\right]\ \frac{225}{\pi^2} \frac{\hbar^2 r_{\mathrm{dH}}^3}{m r^8}, \tag{31}$$

$$\Delta\phi^{\mathrm{b}}(r) = \left[-Z_{\mathrm{d}}^{\mathrm{eff}} \left(1 - \frac{Z_{\mathrm{d}}^{\mathrm{eff}}}{10}\right) r_{\mathrm{dI}}^{3/2} + Z_{\mathrm{dH}} \left(1 - \frac{Z_{\mathrm{dH}}}{10}\right) r_{\mathrm{dH}}^{3/2}\right] \times \left[\frac{12}{n}\right]^{1/2} \frac{28.1}{\pi} \frac{\hbar^2 r_{\mathrm{dH}}^{3/2}}{m r^5}. \tag{32}$$

In eqs (29)–(32), $\Delta\phi^{\mathrm{FE}}(r)$ is the change in the free-electron potential, $\Delta\phi^{\mathrm{c}}(r)$ is the impurity-induced change in s–d hybridization and $\Delta\phi^{\mathrm{b}}(r)$ is due to impurity-induced change in d-bandwidth. It is assumed that due to single impurity, conduction electron density is nearly unchanged. Therefore we use $\kappa' = \kappa$ and $Z_{\mathrm{d}}^{\mathrm{eff}} = Z_{\mathrm{dH}}$ for dilute alloys. For Cr alloys $\kappa' = \kappa = 1.0208$ a.u., for Nb alloys $\kappa' = \kappa = 0.9557$ a.u. and for Mo alloys $\kappa' = \kappa = 0.9771$ a.u. are used in the calculations.

Table 1. The physical parameters of Cr, Nb and Mo metals. a is the lattice parameter, Ω_0 the atomic volume, (in a.u., 1 a.u. = 0.529 Å), Z the number of s and d conduction electrons per atom and A_1, B_1, A_2, B_2 the atomic force constants (in 10^{-3} a.u.) at 1NN and 2NN as defined in eq. (12).

	a	Ω_0	Z	A_1	B_1	A_2	B_2
Cr	5.444	82.5	6	−5.259	2.693	−5.177	1.567
Nb	6.229	120.9	5	7.803	2.000	−3.945	1.685
Mo	5.947	105.2	6	12.168	2.248	−4.548	2.030

Table 2. Potential parameters: Aschroft core radius r_c and d-state radius r_d for impurities (in a.u.), impurity-induced forces F_I and F_{II} (in 10^{-2} a.u.), at the INN's and 2NN's of impurity evaluated using eq. (19) and the impurity-induced relaxation energies E_r (in 10^{-2} eV., 1 a.u. = 27.2 eV) for Cr, Nb and Mo host metals.

			Cr			Nb			Mo		
Impurity	r_c	r_d	F_I	F_{II}	E_r	F_I	F_{II}	E_r	F_I	F_{II}	E_r
V	1.64	1.85	−0.05	0.096	0.025	0.105	0.276	1.004	−0.078	0.247	0.179
Cr	1.55	1.70				0.295	0.356	2.669	−0.019	0.337	0.482
Mn	1.47	1.63	−0.02	0.024	0.008	0.344	0.385	3.720	−0.024	0.369	0.118
Fe	1.34	1.51	−0.06	0.058	0.062	0.425	0.426	4.695	−0.015	0.416	7.554
Zr	2.00	2.67	−0.82	−0.438	4.590	0.146	−0.085	0.039	0.510	−0.129	0.308
Nb	1.91	2.42	0.487	−0.404	3.968				0.310	−0.006	0.216
Mo	1.79	2.27	−0.32	−0.395	0.876	−0.244	0.007	0.151			
Ta	1.93	2.53	0.716	−0.487	7.590	0.030	−0.063	0.008	0.400	−0.065	0.249
W	1.78	2.40	3.073	0.437	75.320	−0.398	−0.146	0.986	0.012	−0.015	0.003

3. Calculations and results

The above formalism is used to calculate the strain field in Cr, Nb and Mo metals due to 3d (V, Cr, Mn, Fe), 4d (Zr, Nb, Mo) and 5d (Ta, W) impurities. The physical parameters and the calculated forces, force constants and relaxation energies are given in tables 1 and 2. The host potential $\phi_{HH}(r)$ and its constituents are shown in figures 1–3. $\phi^{FE}(r)$ and $\phi^{c}(r)$ are repulsive in nature and $\phi^{b}(r)$ is attractive. The minima of $\phi_{HH}(r)$ are at 3.8 a.u., 5.0 a.u. and $r = 4.8$ a.u. for Cr, Nb and Mo metals which are less than the 1NN distances.

The change in potential $\Delta\phi(r)$ due to impurities in Cr, Nb and Mo metal are shown in figures 4–6. In Cr metal, $\Delta\phi(r)$ for 3d impurities Mn and Fe changes from attractive to repulsive and becomes most repulsive at the 1NN. Further its magnitude decreases although it remain repulsive. $\Delta\phi(r)$ for 3d impurity V just shows the opposite behavior. $\Delta\phi(r)$ for 4d impurities Zr, Nb, and Mo changes its character from repulsive to attractive in the vicinity of the 1NN distances. $\Delta\phi(r)$ for 5d impurities Ta and W is similar to that for 4d impurities. In Nb host, $\Delta\phi(r)$ for 3d impurities V, Cr, Mn, Fe changes its sign from attractive to repulsive in the vicinity of 1NN distance and it is most repulsive at the 1NN distance. Although $|\Delta\phi(r)|$ decreases it remains repulsive at all the distances beyond 1NN distances. $\Delta\phi(r)$ for 4d impurity Zr becomes attractive in the vicinity of 1NN distance which is contrary to the other 4d impurity Mo. The behavior of $\Delta\phi(r)$ for 5d impurity Ta is the same as for Zr. However, for W impurity $\Delta\phi(r)$ is attractive. In Mo host, the behavior of $\Delta\phi(r)$

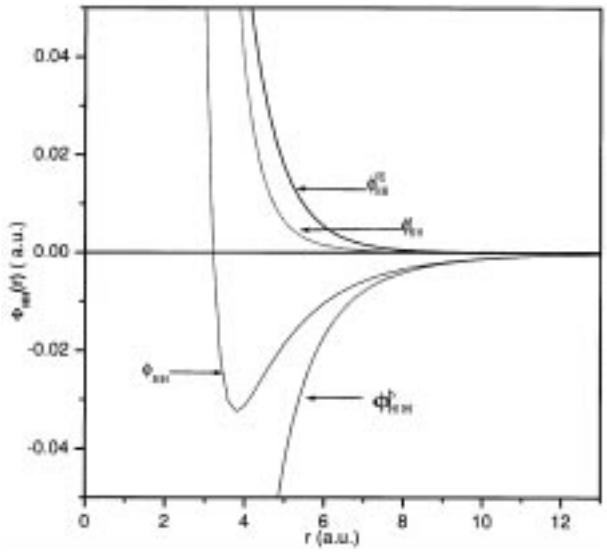

Figure 1. Interatomic potential $\phi_{HH}(r)$ for Cr metal. ϕ^{FE}_{HH} is the free electron contribution, ϕ^{c}_{HH} arises from the shift in the d-band center due to s–d hybridization and ϕ^{b}_{HH} arises from the finite d-bandwidth

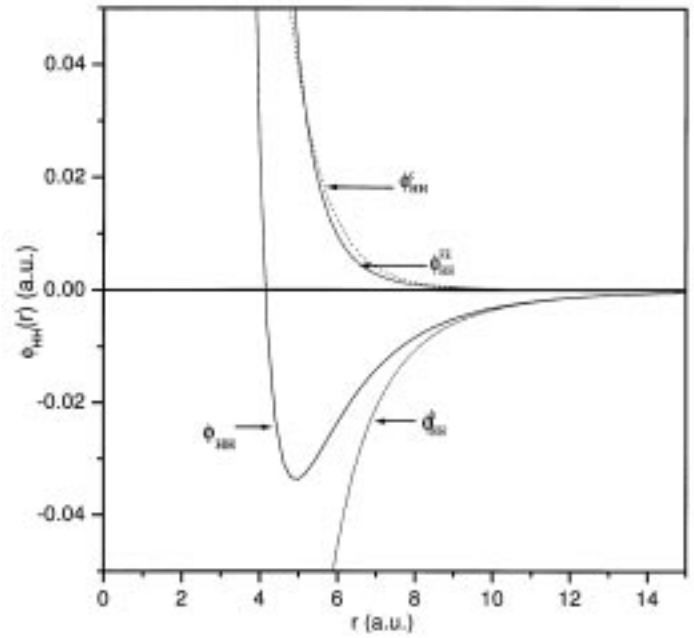

Figure 2. Interatomic potential $\phi_{HH}(r)$ vs. r for Nb. The description of ϕ^{FE}_{HH}, ϕ^{c}_{HH} and ϕ^{b}_{HH} are the same as given in figure 1.

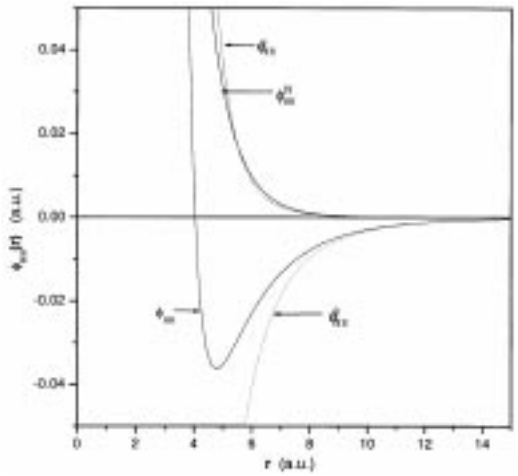

Figure 3. Interatomic potential $\phi_{\mathrm{HH}}(r)$ vs. r for Mo. The description of $\phi_{\mathrm{HH}}^{\mathrm{FE}}$, $\phi_{\mathrm{HH}}^{\mathrm{c}}$ and $\phi_{\mathrm{HH}}^{\mathrm{b}}$ are the same as given in figure 1.

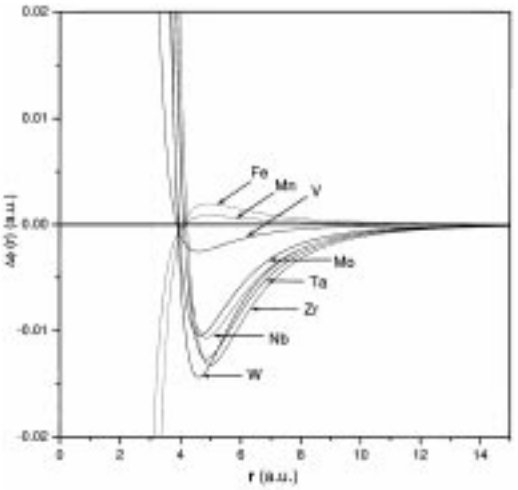

Figure 4. Change in interatomic potential $\Delta\phi(r)$ vs. r for V, Mn, Fe, Zr, Nb, Mo, Ta and W impurities in Cr metal.

for 3d impurities V, Cr, Mn and Fe is the same as that of Nb metal. However, $\Delta\phi(r)$ for 4d and 5d impurities is similar and just opposite to that for 3d impurities. It is changing from repulsive to attractive character and again show the maxima in the vicinity of 1NN and remain attractive beyond the 1NN distance. Further analysis shows that $\Delta\phi(r)$ is quite sensitive to d core radii r_{d} and model potential radii r_c. These parameter are more closer for Zr and Ta and for Mo and W impurities.

The calculated $\Delta\phi(r)$ is used in eq. (19) and F_{I} and F_{II} are calculated, which are given in table 2. In Cr alloys, forces at 1NN distances are attractive for V, Mn, Fe, Zr and

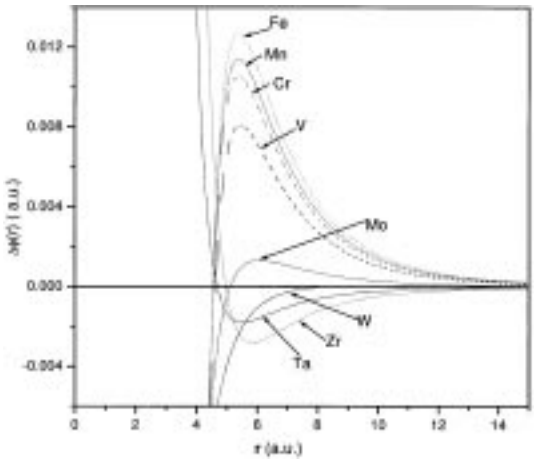

Figure 5. Change in interatomic potential $\Delta\phi(r)$ vs. r for V, Cr, Mn, Fe, Zr, Mo, Ta and W impurities in Nb metal.

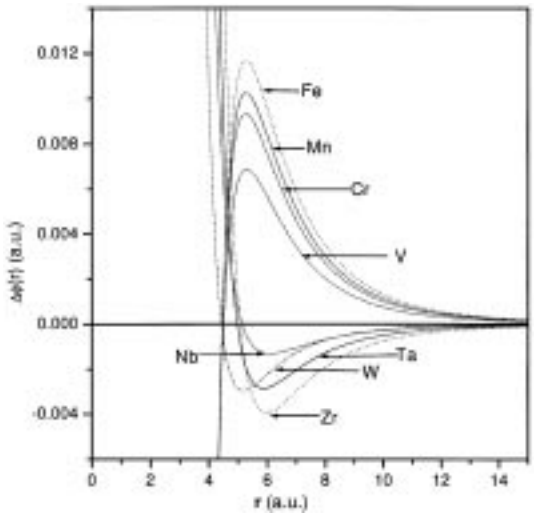

Figure 6. Change in interatomic potential $\Delta\phi(r)$ vs. r for V, Cr, Mn, Fe, Nb, Ta and W impurities in Mo metal.

Mo impurities while repulsive for Nb, Ta and W impurities, whereas the forces at 2NN distance are attractive for Zr, Nb, Mo and Ta impurities and repulsive for V, Mn, Fe and W impurities. $|F_{\mathrm{I}}| < |F_{\mathrm{II}}|$ for V, Mn, Fe, and Mo impurities whereas $|F_{\mathrm{I}}| > |F_{\mathrm{II}}|$ for Zr, Nb, Ta and W impurities. This is consistent with the variation of $\Delta\phi(r)$ for these alloys.

In Nb alloys, the forces are repulsive at the first and second NN's of 3d impurities, i.e., V, Cr, Mn and Fe, the forces are repulsive at the 1NN and attractive at the 2NN's for Zr and

Table 3. Atomic displacements (in 10^{-2} a.u.) of the NN's of V and Mn impurities in Cr metal. (n_1, n_2, n_3) are the coordinates of NN's in units of $(a/2)$ and (u_x, u_y, u_z) are the Cartesian components of atomic displacements in this and subsequent tables. The results are tabulated only to the second decimal points.

NN's	Displacement components					
	V			Mn		
(n_1, n_2, n_3)	u_x	u_y	u_z	u_x	u_y	u_z
111	0.61	0.61	0.61	1.02	1.02	1.02
200	3.83	0.00	0.00	−1.99	0.00	0.00
220	1.07	1.07	0.00	−0.69	−0.69	0.00
311	−0.31	0.34	0.34	0.81	0.20	0.20
222	0.71	0.71	0.71	−0.30	−0.30	−0.30
400	1.08	0.00	0.00	−1.02	0.00	0.00
331	−0.05	−0.05	0.15	0.41	0.41	0.07
420	0.73	0.31	0.00	−0.67	−0.23	0.00
422	0.66	0.31	0.31	−0.50	−0.14	−0.14
511	−0.45	0.10	0.10	0.67	0.05	0.05

Ta impurities while opposite is the behavior for Mo impurity, and for W impurity both F_{I} and F_{II} are attractive. For 3d impurities $|F_{\mathrm{I}}| < |F_{\mathrm{II}}|$, for 4d impurity Zr and 5d impurity W $|F_{\mathrm{I}}| > |F_{\mathrm{II}}|$ while for 4d impurity Ta $|F_{\mathrm{I}}| < |F_{\mathrm{II}}|$. This is again consistent with the character of $\Delta\phi(r)$. In Mo alloys, the forces are attractive at the 1NN distance and repulsive at the 2NN for 3d impurities while they are just opposite in nature for 4d and 5d impurities. In Mo dilute alloys, $|F_{\mathrm{I}}| < |F_{\mathrm{II}}|$ for 3d impurities, $|F_{\mathrm{I}}| > |F_{\mathrm{II}}|$ for 4d, while for 5d impurity Ta $|F_{\mathrm{I}}| > |F_{\mathrm{II}}|$ and for W impurity $|F_{\mathrm{I}}| < |F_{\mathrm{II}}|$.

It is interesting to compare the forces on the same impurities in Cr, Nb and Mo hosts. V, Mn and Fe impurity exert attractive forces at the 1NN and repulsive forces at the 2NN in the Cr and Mo hosts while in Nb, the forces are repulsive. The nature of forces due to Zr impurity is the same in Nb and Mo host and it is different from that in Cr. Ta impurity introduces repulsive and attractive forces at the 1NN and 2NN respectively in all the three hosts, while the forces due to W impurity are at variance in all the three hosts. The magnitude of forces due to 3d impurities is larger in Nb host while forces for 4d and 5d impurities is large in the Cr host.

These values of F_{I} and F_{II}, and the calculated values of the force constants A_1, B_1, A_2 and B_2 are used to calculate $\phi_{\alpha\alpha}(\vec{q})$ and $\phi_{\alpha\beta}(\vec{q})$and hence $\vec{Q}(\vec{q})$ with the help of eq. (9). The inverse Fourier transform of $\vec{Q}(\vec{q})$, as given in eq. (10) gives $\vec{u}(\vec{R}_n^0)$. The numerical calculations are carried out replacing summation by integration and using the fact that, for any function $F(q)$

$$\int_{BZ} F(q)\,\mathrm{d}q = \frac{1}{4}\int_{\mathrm{cube}} F(q)\,\mathrm{d}q \tag{33}$$

where the cube inscribes the first Brillouin zone (BZ). The cubic symmetry of the lattice is retained in this integration procedure, although the exact anisotropy of Brillouin zone is not there. This may not introduce serious error considering other simplifications in the calculations. These calculated values of atomic displacements are given in tables 3–14 up to ten nearest neighbors of impurity.

Table 4. Atomic displacements (in 10^{-2} a.u.) of the NN's of Fe and Zr impurities in Cr metal.

NN's	Displacement components					
	Fe			Zr		
(n_1,n_2,n_3)	u_x	u_y	u_z	u_x	u_y	u_z
111	2.88	2.88	2.88	24.09	24.09	24.09
200	−5.16	0.00	0.00	−1.22	0.00	0.00
220	−1.80	−1.80	0.00	−2.69	−2.69	0.00
311	2.22	0.59	0.59	11.93	6.73	6.73
222	−0.76	−0.76	−0.76	1.05	1.05	1.05
400	−2.74	0.00	0.00	−8.76	0.00	0.00
331	1.13	1.13	0.21	6.95	6.95	2.66
420	−1.79	−0.60	0.00	−5.46	−1.29	0.00
422	−1.32	−0.37	−0.37	−3.02	0.18	0.18
511	1.83	0.14	0.14	8.18	1.76	1.76

Table 5. Atomic displacements (in 10^{-2} a.u.) of the NN's of Nb and Mo impurities in Cr metal.

NN's	Displacement components					
	Nb			Mo		
(n_1,n_2,n_3)	u_x	u_y	u_z	u_x	u_y	u_z
111	−23.73	−23.73	−23.73	6.43	6.43	6.43
200	39.28	0.00	0.00	12.34	0.00	0.00
220	13.88	13.88	0.00	3.02	3.02	0.00
311	−17.78	−5.02	−5.02	1.18	2.33	2.33
222	5.67	5.67	5.67	2.51	2.51	2.51
400	21.48	0.00	0.00	1.93	0.00	0.00
331	−9.08	−9.08	−1.81	1.11	1.11	0.98
420	14.00	4.62	0.00	1.41	0.77	0.00
422	10.23	2.79	2.79	1.61	1.03	1.03
511	−14.52	−1.22	−1.22	0.03	0.64	0.64

The results for 3d impurities V, Mn, Zr and Fe in Cr host are given in tables 3 and 4. For V impurity the first 3NN's displaces away from the impurity, 4th NN's have anisotropic displacements, 5NN's and 6NN's displace away from the impurity and then the displacements show oscillatory behavior. For Mn and Fe impurities, 1NN's displace away from impurity and 2NN's and 3NN's displace towards the impurity atom and then the displacements exhibit oscillatory behavior. The results for 4d impurities Zr, Nb, and Mo are given in tables 4 and 5. For the Zr impurity, the 1NN's displace away from the impurity and next two NN's move towards the impurity, and 4NN's and 5NN's displace away from the impurity and further the magnitude of displacements of the NN's decreases with oscillatory behavior. For the Nb impurity, the 1NN's displace towards the impurity and next two NN's move away from the impurity while 4NN's show the contraction. For the Mo impurity nearly all the NN's get displaced away from the impurity. However the magnitude of displacements decreases and it is oscillatory in nature. The results for 5d impurities Ta and W are given in table 6. For Ta impurity 1NN's show contraction towards the impurity, next two NN's show expansion away from the impurity, and 4NN's further show the lattice

Table 6. Atomic displacements (in 10^{-2} a.u.) of the NN's of Ta and W impurities in Cr metal.

NN's	Displacement components					
	Ta			W		
(n_1,n_2,n_3)	u_x	u_y	u_z	u_x	u_y	u_z
111	−33.38	−33.38	−33.38	107.67	107.67	107.67
200	51.53	0.00	0.00	−74.72	0.00	0.00
220	18.42	18.42	0.00	−32.44	−32.44	0.00
311	−24.41	−7.21	−7.21	64.29	27.14	27.14
222	7.33	7.33	7.33	−7.52	−7.52	−7.52
400	28.96	0.00	0.00	−62.54	0.00	0.00
331	−12.55	−12.55	−2.62	35.13	35.13	10.41
420	18.85	6.18	0.00	−40.08	−11.86	0.00
422	13.68	3.64	3.64	−26.69	−4.60	−4.60
511	−19.79	−1.77	−1.77	48.31	6.93	6.93

Table 7. Atomic displacements (in 10^{-2} a.u.) of the NN's of V and Cr impurities in Nb metal.

NN's	Displacement components					
	V			Cr		
(n_1,n_2,n_3)	u_x	u_y	u_z	u_x	u_y	u_z
111	15.40	15.40	15.40	21.84	21.84	21.84
200	28.66	0.00	0.00	41.22	0.00	0.00
220	5.49	5.49	0.00	7.53	7.53	0.00
311	4.14	−2.47	−2.47	6.59	−2.46	−2.46
222	3.34	3.34	3.34	4.00	4.00	4.00
400	−0.90	0.00	0.00	−3.27	0.00	0.00
331	0.65	0.65	9.51	0.52	0.52	13.37
420	4.43	−6.96	0.00	6.08	−7.76	0.00
422	−1.47	4.90	4.90	−1.61	7.01	7.01
511	5.48	2.97	2.97	6.21	4.45	4.45

contraction, further NN's displacements are oscillatory. For W impurity, 1NN's displace away from the impurity and next two NN's show the lattice contraction and after that the displacements follow the oscillatory behavior.

The magnitude of the atomic displacements, for the first 5NN's in Cr alloys are shown in figure 7. The impurities except V and Mn shows maximum displacement at the 1NN's. The V and Mn impurities show maximum displacements at 2NN's. The maximum strain is obtained for CrW alloy, which shows the average displacement of 5.4% of R_1^0, whereas the minimum displacement of 0.36% of R_1^0 is found for CrV. The displacements in CrW alloy are large due to large external force at 1NN due to W impurity which depends on the slope of the excess potential $\Delta\phi(r)$ due to W impurity. We find that the strain field increases for the 3d and 5d impurities with the atomic number, whereas such a trend is not found for 4d impurities.

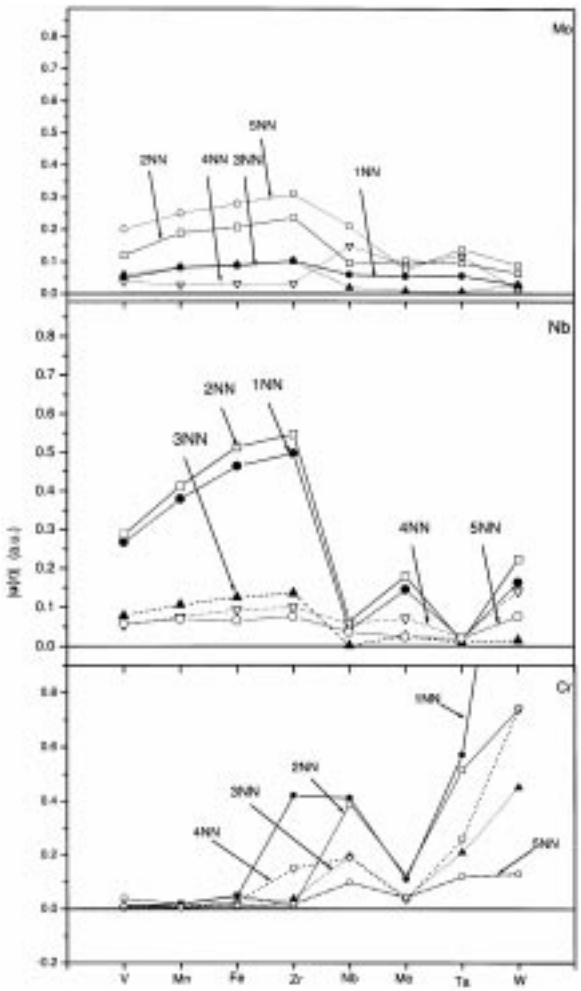

Figure 7. Magnitude of the displacements $|u(r)|$ as a function of atomic number of the impurities in Cr, Nb and Mo metals. The lines joining the points are for visual guidance.

The results for atomic displacements due to 3d impurities V, Cr, Mn and Fe in Nb are given in tables 7 and 8. For all these impurities, the first 3NN's are displaced away from the impurity while the displacements of 4NN's are asymmetric. Fifth NN's are displaced away from the impurity and the 6NN get attracted towards the impurity. Beyond this the oscillatory behavior of the displacements continues. The results for Zr, Mo, Ta and W impurities in Nb are given in tables 9 and 10. For Zr impurity the first two NN's are displaced away from the impurity, third NN's get attracted towards the impurity, 4NN's get repelled and than the asymmetric oscillatory behavior of displacements continue. The first 4NN's of Mo impurity in Nb host get attracted towards the impurity, the 5NN's and 6NN's get repelled away from the impurity and then the displacements are asymmetric and

Table 8. Atomic displacements (in 10^{-2} a.u.) of the NN's of Mn and Fe impurities in Nb metal.

NN's	Displacement components					
	Mn			Fe		
(n_1,n_2,n_3)	u_x	u_y	u_z	u_x	u_y	u_z
111	26.78	26.78	26.78	28.65	28.65	28.65
200	51.35	0.00	0.00	54.69	0.00	0.00
220	8.83	8.83	0.00	9.56	9.56	0.00
311	9.16	−1.45	−1.45	9.49	−2.00	−2.00
222	3.81	3.81	3.81	4.39	4.39	4.39
400	−6.98	0.00	0.00	−6.61	0.00	0.00
331	0.03	0.03	16.21	0.21	0.21	17.39
420	7.15	−6.37	0.00	7.74	−7.72	0.00
422	−1.26	8.69	8.69	−1.56	9.27	9.27
511	5.27	5.80	5.80	6.32	6.11	6.11

Table 9. Atomic displacements (in 10^{-2} a.u.) of the NN's of Zr and Mo impurities in Nb metal.

NN's	Displacement components					
	Zr			Mo		
(n_1,n_2,n_3)	u_x	u_y	u_z	u_x	u_y	u_z
111	2.35	2.35	2.35	−8.33	−8.33	−8.33
200	6.35	0.00	0.00	−17.92	0.00	0.00
220	−0.12	−0.12	0.00	−1.80	−1.80	0.00
311	3.22	3.39	3.39	−5.41	−3.29	−3.29
222	−2.13	−2.13	−2.13	1.43	1.43	1.43
400	−7.30	0.00	0.00	9.28	0.00	0.00
331	−1.36	−1.36	1.01	1.44	1.44	−4.60
420	−0.04	6.53	0.00	−1.51	−5.55	0.00
422	1.49	0.98	0.98	−1.30	−2.93	−2.93
511	−4.79	1.29	1.29	3.94	−2.63	−2.63

oscillatory. The same characteristic of atomic displacements is found due to Ta and W impurities.

The magnitude of the atomic displacements of the first 5NN's of all the transition metal impurities in Nb are compared in figure 7. Except for Ta impurity, the 2NN's are displaced more than the 1NN's. The atomic displacements for 3d impurities from V to Fe, 4d impurities Zr to Mo and 5d impurities Ta to W are in increasing order. The strain is found maximum for NbFe alloy and minimum for NbTa alloy. In NbFe the first, second and third NN's are displaced by 9.2%, 10.1% and 2.5% of R_1^0 respectively, while these displacements for NbTa alloy are 0.32%, 0.22% and 0.18% respectively. The average atomic displacements of first 2NN's in NbZr alloy is 0.052 a.u., while the analysis of XAFS spectra predict about 0.10 ± 0.01 a.u. [12]. Considering all the approximations in the calculation and in the analysis of the experimental data these results are of the same order.

The results for atomic displacements in Mo alloys are tabulated in tables 11–14. For 3d impurities V, Cr, Mn and Fe, the first two NN's get displaced away from the impurity, third and fourth NN's shift towards the impurity and then the next three NN's get displaced away

Table 10. Atomic displacements (in 10^{-2} a.u.) of the NN's of Ta and W impurities in Nb metal.

NN's	Displacement components					
	Ta			W		
(n_1,n_2,n_3)	u_x	u_y	u_z	u_x	u_y	u_z
111	−0.98	−0.98	−0.98	−9.37	−9.37	−9.37
200	−1.13	0.00	0.00	−22.22	0.00	0.00
220	−0.69	−0.69	0.00	−1.02	−1.02	0.00
311	0.66	1.50	1.50	−8.80	−7.65	−7.65
222	−1.15	−1.15	−1.15	4.38	4.38	4.38
400	−2.50	0.00	0.00	17.94	0.00	0.00
331	−0.56	−0.56	−0.76	3.15	3.15	−4.71
420	−0.54	3.15	0.00	−0.94	−14.19	0.00
422	0.70	−0.23	−0.23	−3.26	−3.54	−3.54
511	−2.36	0.11	0.11	10.34	−3.83	−3.83

Table 11. Atomic displacements (in 10^{-2} a.u.) of the NN's of V and Cr impurities in Mo metal.

NN's	Displacement components					
	V			Cr		
(n_1,n_2,n_3)	u_x	u_y	u_z	u_x	u_y	u_z
111	2.78	2.78	2.78	4.68	4.68	4.68
200	11.85	0.00	0.00	19.02	0.00	0.00
220	−4.16	−4.16	0.00	−5.82	−5.82	0.00
311	−3.68	−0.58	−0.58	−2.57	−0.66	−0.66
222	11.66	11.66	11.66	14.75	14.75	14.75
400	2.42	0.00	0.00	4.87	0.00	0.00
331	1.99	1.99	4.29	2.63	2.63	5.32
420	−6.03	3.15	0.00	−6.87	6.51	0.00
422	5.14	−10.38	−10.38	6.52	−13.18	−13.18
511	6.12	−2.78	−2.78	6.37	−2.42	−2.42

and then the oscillatory behavior continues. The 4d impurity Zr creates dilation up to first 4NN's and then the contraction and dilation oscillatory behavior of displacements continues. However, the Nb impurity dilates the first two NN's, third NN's get contracted and then the rapid oscillatory behavior of atomic displacement is found. The 5d impurity Ta displaces the host atoms on the same pattern as Zr impurity. However, the displacement pattern by W impurity is different. The first two NN's shift towards the impurity, next two NN's get displaced away from the impurity and then the oscillatory behavior of the displacements continues.

The magnitudes of the atomic displacements of the first 5NN's in Mo alloys are shown in figure 7. As $|F_{\mathrm{II}}| > |F_{\mathrm{I}}|$ for 3d impurities (V, Cr, Mn and Fe) the displacements are minimum at the 4NN's and maximum at the 5NN's. However, the displacements due to 4d and 5d impurities are more oscillatory. The maximum strain is found for MoFe alloy, where the 1NN's are displaced by 1.96%, 2NN by 4.6%, 3NN by 1.97%, 4NN by 0.6% and 5NN by 6.1% of R_1^0. W impurity produces minimum strain where the 1NN's are displaced by 0.52%, 2NN's by 1.2%, 3NN by 0.54%, 4NN by 0.21% and 5NN by 1.7% of R_1^0.

Table 12. Atomic displacements (in 10^{-2} a.u.) of the NN's of Mn and Fe impurities in Mo metal.

NN's	Displacement components					
	Mn			Fe		
(n_1, n_2, n_3)	u_x	u_y	u_z	u_x	u_y	u_z
111	5.08	5.08	5.08	5.85	5.85	5.85
200	20.69	0.00	0.00	23.75	0.00	0.00
220	−6.37	−6.37	0.00	−7.21	−7.21	0.00
311	−2.91	−0.73	−0.73	−2.97	−0.81	−0.81
222	16.18	16.18	16.18	18.12	18.12	18.12
400	5.26	0.00	0.00	6.15	0.00	0.00
331	2.88	2.88	5.84	3.24	3.24	6.53
420	−7.57	7.03	0.00	−8.37	8.24	0.00
422	7.15	−14.46	−14.46	8.01	−16.20	−16.20
511	7.05	−2.71	−2.71	7.70	−2.87	−2.87

Table 13. Atomic displacements (in 10^{-2} a.u.) of the NN's of Zr and Nb impurities in Mo metal.

NN's	Displacement components					
	Zr			Nb		
(n_1, n_2, n_3)	u_x	u_y	u_z	u_x	u_y	u_z
111	3.36	3.36	3.36	3.10	3.10	3.10
200	9.50	0.00	0.00	10.02	0.00	0.00
220	1.29	1.29	0.00	−0.48	−0.48	0.00
311	15.16	0.97	0.97	8.78	0.45	0.45
222	−12.16	−12.16	−12.16	−4.26	−4.26	−4.26
400	7.25	0.00	0.00	5.53	0.00	0.00
331	−1.50	−1.50	−5.09	−0.35	−0.35	−1.97
420	10.42	10.44	0.00	4.91	7.86	0.00
422	−5.30	10.56	10.56	−1.84	3.62	3.62
511	−13.78	8.86	8.86	−7.10	4.93	4.93

A comparison of the displacements due to impurities in Cr, Nb and Mo hosts in figure 7 shows that the displacements due to 3d impurities in Cr host are smaller than those in Nb and Mo hosts due to 4d and 5d impurities, whereas displacements due to 3d impurities are more due to 4d and 5d impurities in Nb and Mo hosts, and within Nb and Mo hosts, the atomic displacements in Nb host are nearly twice the magnitude to that of Mo host.

The calculated displacements up to 2NN's are used to evaluate the impurity-induced relaxation energy E_{r} which is given as

$$E_{\mathrm{r}} = -\frac{1}{2}\sum_{n\alpha} F_{n\alpha} u_{n\alpha}. \tag{34}$$

Here $\vec{F}$ is the isotropic impurity force and F_{I} and F_{II} tabulated in table 2 are used. The results for E_{r} are also given in table 2. The relaxation energy of 3d impurities V, Mn, and Fe in Cr are smaller than in Nb and Mo hosts. Therefore 3d impurities may easily be dissolved in Cr. The relaxation energy of 4d impurities is maximum in Cr and minimum in Nb and for

Table 14. Atomic displacements (in 10^{-2} a.u.) of the NN's of Ta and W impurities in Mo metal.

NN's	Displacement components					
	Ta			W		
(n_1,n_2,n_3)	u_x	u_y	u_z	u_x	u_y	u_z
111	3.16	3.16	3.16	−1.54	−1.54	−1.54
200	9.55	0.00	0.00	−6.31	0.00	0.00
220	0.39	0.39	0.00	1.98	1.98	0.00
311	11.67	0.69	0.69	1.03	0.23	0.23
222	−7.98	−7.98	−7.98	−5.10	−5.10	−5.10
400	6.24	0.00	0.00	−1.57	0.00	0.00
331	−0.90	−0.90	−3.43	−0.90	−0.90	−1.85
420	7.46	8.93	0.00	2.43	−2.09	0.00
422	−3.47	6.89	6.89	−2.25	4.56	4.56
511	−10.17	6.72	6.72	−2.29	0.91	0.91

5d impurities it is minimum in Mo and maximum in Cr. Therefore, it is concluded that 4d impurities are more easily dissolved in Nb than in Cr or Mo whereas the 5d impurities are easily dissolved in the Mo and are difficult to dissolve in Cr. Further, the relaxation energies for 3d impurities in Mo are less than those in Nb except for Fe. Therefore V, Cr and Mn may more easily be dissolved in Mo than in Nb while Fe may more easily be dissolved in Nb. The relaxation energies for Zr, Mo and Ta in Nb are smaller by an order of magnitude than those for V, Cr, Mn, Fe and W impurities. This is due to smaller displacements due to these impurities. Again the relaxation energies are minimum for Mn in Cr, for W in Mo and for Ta in Nb.

4. Discussion and summary

The strain field due to 3d, 4d and 5d impurities in 3d (Cr) and 4d (Nb and Mo) host metals are calculated using Kazaki lattice static method for the harmonic lattice. Wills and Harrison [7] model potential is used for the host Cr, Nb and Mo metals and the impurities, Thomas–Fermi screening is used for s electron and bound state screening is used for d electrons which is justified in the tight-binding description of transition metals. Both the host potential $\phi_{\mathrm{HH}}(r)$ and change in potential $\Delta\phi(r)$ are small and smooth beyond 2NN distance. Therefore the contribution to $\phi_{\alpha\beta}(q)$ and $F_\alpha(q)$ is expected to be small beyond 2NN's. It is found that the same impuriy behaves differently in 3d and 4d host metals due to the change in d-character of host metals. The strain field due to 3d impurities is least in Cr metal, while it is larger in Nb and Mo metals. Similar trend is found for relaxation energies also. Therefore 3d impurities may be more easily dissolved in Cr than in Nb or Mo. For 4d and 5d impurities the strain field and relaxation energy is larger in Cr metal, than in Nb and Mo hosts. Therefore 4d and 5d impurities may be easily dissolved in Nb and Mo. The tabulated values of atomic displacements will be quite useful to investigate heat of sloution, electric field gradients, asymmetry parameter, wipe out number, Knight shift and for all the properties of the defect lattice where impurity induced displaced positions of the host atoms in dilute alloys of Cr, Nb and Mo are needed.

Acknowledgement

The financial support from University Grant Commission (UGC), New Delhi is gratefully acknowledged.

References

[1] John A Shields Jr., *Molybdenum and its alloys, advanced materials and processes* **142**, 28 (1992)
[2] G Patern, S Barbanera and F Murtas, *IEEE Trans. Appl. Superc.* **3**, 1253 (1993)
[3] K H Miska, M Semchysen and E P Whelan (eds), *Cilmax specialty metals* (Cleveland, OH, 1985) p. 107
[4] J Singh, P Singh, S K Rattan and S Prakash, *Phys. Rev.* **B49**, 932 (1994)
[5] Hitesh Sharma and S Prakash, *Symposium on disordered materials*, Chandigarh, 2001 (Proceeding to be published in Narosa Publication 2002)
[6] Hitesh Sharma and S Prakash, *Phys. Rev.* **B**, communicated
[7] J M Wills and W A Harrison, *Phys. Rev.* **B28**, 4363 (1983)
[8] W Hanke, *Phys. Rev.* **B8**, 4585 (1973); **B8**, 4591 (1973)
[9] J Singh, N Singh and S Prakash, *Phys. Rev.* **B12**, 3159 (1975)
[10] J Singh and S Prakash, *Nuovo Cimento* **B37**, 131 (1977)
[11] H Kanzaki, *J. Phys. Chem. Solids* **2**, 24 (1957)
[12] U Scheuer and B Lengeler, *Phys. Rev.* **B44**, 9883 (1991)